

Experimental Investigation of Conical Spring Inserts on In-Tube Heat Transfer and Pressure Drop

Muhammet Kaan
YEŞİLYURT¹
Ömer ÇOMAKLI²

¹Department of Machine and Metal Technologies, Atatürk University, Vocational School of Technical Sciences, Erzurum, Turkey

²Department of Mechanical Engineering, Atatürk University, Faculty of Engineering, Erzurum, Turkey

ABSTRACT

Two-phase flow is preferred in many industrial applications where high heat flux is present and/or required because of its higher heat transfer coefficient compared to single-phase flows. However, there are some adverse effects that will reduce the life of the system and its components, as well as risk the safe operation and its benefits. In this study, the effects of conical coiled springs as an in-tube element aimed at the elimination, or actually minimization, of said adverse effects are investigated experimentally. In this study, a 2-phase flow system was used, with the test section comprised of a straight horizontal tube with forced convection boiling. The effects of equally spaced conical spring arrays having different pitches as an in-tube heat transfer enhancement element on heat transfer and pressure drop in 2-phase flow were investigated. Fluid supply flow rate and pitches of conical springs inserted into the tube were selected as study parameters, and experiments were made under constant operating pressure, constant inlet temperature, constant heat input, and fixed outlet restrictions to investigate the effects of conical springs. Four different heat transfer surface configurations are used. Experiments showed that the minimum point shifted to the right on the curve with the increase in heat input, and the mass flow rate at a given pressure drop observed is directly proportional to the thermal power. The highest pressure drop in the 2-phase flow region is observed with tube 4 (10 mm pitch) and tube 3 (20 mm pitch), while the lowest pressure drop is with tube 1.

Keywords: Conical spring insert, heat transfer, pressure drop, 2-phase flow

INTRODUCTION

Nuclear reactors, cooling systems, steam generators, processing facilities, and similar industrial operations commonly involve 2-phase flows.¹ These flows occur in various natural phenomena, from the formation of raindrops within clouds to the behavior of water during ice formation. The higher heat transfer coefficients of 2-phase flows compared to single-phase flows, coupled with the increasing industrial demand for high heat flux applications, have led to a rapid growth in interest and research in this field.

In many industrial systems where heat transfer occurs through boiling, flow instabilities due to fluctuations in system pressure and fluid flow can result in disruptions and failures, significantly reducing the economic lifespan of these systems. These flow instabilities can lead to issues such as thermal fatigue, boiling crises, mechanical vibrations, difficulty in control due to high transient temperatures, and burn-out events on the heat transfer surfaces.²

The economic design, optimization, and safe operation of these systems are directly linked to their ability to predict the thermal characteristics and hydrodynamic instabilities of 2-phase flows. Two-phase flows involve the formation of interfaces between phases, and the shapes these interfaces take are fundamental in defining the characteristics of the 2-phase flow. The flow direction significantly influences the shapes of these interfaces, categorizing 2-phase flows into inclined, vertical, and horizontal based on flow direction. Each of these flow directions exhibits distinct flow regimes and characteristics. The influence of gravity, according to the flow direction, leads to a fundamental categorization, with horizontal flow systems experiencing phase separation due to the perpendicular effect of gravity. In these systems, lower-density vapor is found in the upper portion of the tube, and higher-density liquid is in the lower section. The lower heat transfer coefficient in the vapor phase compared to the liquid phase in the carrying systems results in the occurrence of a phenomenon known as “burn-out” in the upper regions.³

Received: 02.11.2023

Accepted: 04.12.2023

Publication Date: 31.12.2023

Corresponding author:
Muhammet Kaan YEŞİLYURT
E-mail: kaan.yesilyurt@atauni.edu.tr

Cite this article as: Yeşilyurt MK, Çomaklı Ö. Experimental investigation of conical spring inserts on in-tube heat transfer and pressure drop. *NanoEra* 2023;3(2):40-52.



Content of this journal is licensed under a Creative Commons Attribution-NonCommercial-NoDerivatives 4.0 International License.

Naturally, the effect of gravity on flow systems in vertical and inclined flows results in fewer variations in the shapes of the interfaces compared to horizontal flows. Hence, the factors influencing flow regimes are the absolute and relative flow rates of the 2 phases, system geometry, and the forces acting on each phase. Two types of instability are identified in 2-phase flow systems: “static” and “dynamic.” “Static instabilities” refer to a situation where a small change in flow conditions in a stable state leads to an asymptotic shift in the working regime, illustrated by phenomena such as boiling crises and flow excursions. “Dynamic instabilities” occur when the process is significantly influenced by inertia and other feedback effects. These instabilities happen because the flow’s inertia and the 2-phase mixture’s ability to be compressed do not interact well enough. There are also many feedback loops that involve changes in flow rate, pressure drop, and density in the channel where boiling happens. Dynamic instabilities are classified into 4 main categories: (i) pressure drop oscillations (PDO), (ii) thermal oscillations in tubes causing thermal fatigue due to significant temperature changes on the tube wall, (iii) density-wave oscillations, which have amplitudes smaller than pressure drop oscillations and equal to the transit time of the fluid, and (iv) high-frequency acoustic oscillations.^{4,5}

In an effort to enhance heat transfer, options are using active systems, which require external power sources, and passive systems, which leverage geometric changes, arrangements, or modifications (e.g., treated surfaces, rough surfaces, swirling flow devices) without external power.⁶ One commonly explored approach is manipulating the flow regime within the system to improve heat transfer. Enhanced heat transfer, in turn, boosts the operational efficiency of these systems, leading to the development of more compact systems, reduced installation space requirements,⁷ decreased initial costs, and shorter payback periods.

Methods for manipulating the flow regime and enhancing heat transfer characteristics vary depending on the system and its structural design. These methods encompass inserting devices within tubes or channels and attaching components at the inlet, outlet, or along the flow path. Studies typically employ numerical and experimental methods, often using a circular single tube as the test section with an insert (such as a swirl/vortex generator or turbulator) to induce turbulent flow.⁸⁻¹⁶

A review of the literature on 2-phase flow systems reveals numerous studies that have investigated heat transfer improvement using inserts, turbulators, and swirl/vortex generators. These turbulators can take various forms, including blades,¹⁷ rods,^{18,19} rings,^{20,21} tapes,^{13,22} strips,^{13,23} or coils.^{24,25} These turbulators enhance heat transfer by promoting flow mixing, resulting in turbulent flow induced by longitudinal vortices. Several parameters impact the enhancement rate achieved by turbulators, including their shape, geometry, placement, spacing or pitch, flow attack angle, material, effective diameter, Reynolds number, and additional modifications such as perforations or wings.²⁶

In the early 20th century, alongside the industrial revolution and the rapid development of industrial applications, research on 2-phase flows and their related issues significantly increased. Since Lorentz’s pioneering experimental investigation of the hydrodynamics of 2-phase flows in 1909, numerous studies have been conducted in this field.

Among these studies, Ledinegg’s 1938 research on flow instabilities in heated parallel steam generator channels, later known

as “Ledinegg instability,” is of particular importance. Ledinegg observed that the characteristic curve of the flow, which should always have a positive slope in single-phase flow, exhibited negative slopes in certain flow rate ranges. This observation indicated that there was not a single flow rate corresponding to a single pressure drop, leading to the system transitioning between stable states.

In 1956, Davidov²⁷ conducted experimental research by providing heat flux to test tubes using electrical power, examining oscillations. He observed that the periods of these oscillations were almost equal to the transit time of the fluid in the test tube. The research also revealed that extending the portion exposed to excessive cooling and connecting the channels increased system stability, while using restrictive elements at the outlet of the test tube reduced stability.

Stenning and Veziroğlu,²⁸ using R-11 as the working fluid, identified and defined 3 different types of dynamic instabilities in their experimental study. These included “density change oscillations” resulting from the movement of high- and low-density fluid waves along the heated channel, “pressure drop oscillations” causing large-amplitude oscillations in pressure, wall temperature, and fluid flow rate, and “thermal oscillations” related to the instability of the liquid film layer on the channel wall. The research also indicated that the presence of a compressible volume in front of the test section was necessary for pressure drop oscillations to occur. Then, Veziroğlu and Lee²⁹⁻³¹ compared their experimental results on pressure drop and density change oscillations with earlier research on horizontal channels using R-11 in a vertical upflow system. They found that vertical upflow systems were more stable than horizontal flow systems.

Aritomi et al³²⁻³⁴ developed a nonlinear mathematical model for flow instability based on experimental work in a vertically upward parallel channel system with forced convection, boiling, and water as the working fluid. The model was compared to experimental data from a 2-parallel channel system and was found to be in good agreement. The model was later applied to systems with 3 and 4 parallel channels. Aritomi et al³³ also examined density change oscillations and the effects of slip ratio on stability in parallel boiling systems using both experimental and a new, more complex analytical model. They explored the factors influencing oscillations and the movement of the boiling boundary in low heat flux and high inlet subcooling conditions.

Kakac et al³⁵ did experiments and used a homogeneous 2-phase flow model to figure out how to measure thermal oscillations in an R11-based vertically upward single forced-convection channel test system. They investigated the effects of fluid inlet temperature, heat power, and heating tube dimensions on thermal oscillations. They observed density change, pressure drop, and thermal oscillations. The applied model involved one-dimensional flow equations and expressed the conditions for the emergence of thermal oscillations. The theoretical results were consistent with experimental findings in terms of oscillations, amplitudes, and period values. Thermal oscillations were observed parallel to pressure drop oscillations, but the maximum values of pressure drop oscillations shifted away from the maximum values of thermal oscillations with a phase lag.

Padki et al³⁶ developed a new integral formulation based on dynamic system theory and derived pressure drop, Ledinegg instability’s stability criteria, and mass flow characteristics from

the negative slope of the pressure drop stability region. Differences between pressure drop and Ledinegg instability reflected bifurcation-type differences.

Ding et al³⁷ observed that the amplitude of inlet pressure oscillations in a horizontal boiling tube system decreased as the mass flow rate decreased. It increased as the inlet temperature value rose or the inlet subcooling degree decreased. The periods were directly proportional to the mass flow rate and inlet subcooling degree. Density change oscillations were observed in the negative slope region, and thermal oscillations always accompanied pressure drop oscillations and were observed on the upper side of the tube wall.

Xiao et al³⁸ found that density change oscillations were more pronounced in high-pressure parallel channel systems than in single channels, both in their analytical model and experimental investigation.

Liu et al^{39,40} experimentally examined flow transition boiling, thermal oscillations, and hydrodynamic instabilities in a vertically oriented, boiling, forced-convection, vertical tube test system using R-12 as the working fluid. They observed 2 distinct oscillation models in the boiling zones of flow transition, one with high frequency and low amplitude and the other with low frequency and high amplitude. They identified the low-frequency model parameters, which included heated wall capacity, axial heat conduction gradient, and boiling characteristics.

Guo et al⁴¹ examined how 2-phase flow, pressure drop oscillations, and their boundaries affected transient heat transfer in a spiral tube with 2-phase steam–water flow. They conducted experiments using unsaturated water flow and 2-phase steam–water flow to investigate local heat transfer with non-uniform features. The study analyzed the effects of secondary flow, flow oscillations, and their interactions. Peripheral time-averaged Nusselt numbers were significantly different between local and vibrating flow. The study also discussed pressure drop oscillations and their boundaries for steam–water 2-phase flow in a spirally heated tube. The effects of parameters such as friction, heating conditions, and other variables on the pressure drop oscillations were investigated.

Çomaklı et al⁴² studied 2-phase flow instabilities in a horizontal boiling straight tube system with a fixed system pressure and constant heat flux. They observed that dynamic instabilities of all types occurred at all temperature values. The stability boundaries shifted toward lower mass flow rates as the inlet temperature decreased, indicating that system instability increased with increasing inlet temperature. The periods of pressure drop and density change oscillations changed directly with the mass flow rate and inversely with the inlet temperature value. The study emphasized the importance of channel length as a significant parameter concerning dynamic 2-phase flow instabilities.

Yu et al⁴³ investigated 2-phase pressure drop, boiling heat transfer, and critical heat flux in a horizontal tube system with a length of 0.91 m and an inner diameter of 2.98 mm. They successfully related the results of pressure drop and heat transfer coefficient to changes in existing correlations for both small channels with cooling fluids and larger channels with water. In smaller channels, the pressure drop in 2-phase flow was observed to be lower than expected for the same mass flow rates. A comparison was made with the Chisholm correlation, and differences were attributed to differences in 2-phase flow regimes between channel

sizes. The Chisholm correlation for smaller channels was modified to improve prediction accuracy, and it was observed that the heat power significantly affected boiling heat transfer in small channels.

Salman et al⁴⁴ conducted a numerical study comparing the heat transfer and friction factors of V-cut twisted tape inserts with classical twisted tape inserts at various twist ratios. They found that the heat transfer enhancement was positively related to the Reynolds number and inversely related to the twist ratio. V-cut twisted tape inserts with a twist ratio of 2.93 and a cut depth of 0.5 cm achieved the highest heat transfer rate. V-cut twisted tape inserts also offered better heat transfer performance compared to right-left helical tape inserts, resulting in an overall maximum heat transfer enhancement of 107%. Alam et al.⁴⁵ presented a comprehensive literature review of turbulators in air ducts, highlighting that perforations in ribs, chambers, and blocks, as well as a combination of rib and delta fins, demonstrated improved thermo-hydraulic performance in solar air heaters and heat exchangers.

Razzaghi et al.⁴⁶ studied heat transfer in elliptic tubes arranged in staggered bundles with aluminum foam porous media inserts. Despite higher pressure drops at higher Reynolds numbers, they found that the use of aluminum foams significantly improved heat transfer. Altering pitch arrangements in laminar flow regimes effectively increased overall efficiency.

Zheng et al¹⁸ numerically studied the effect of rod-type vortex generator inserts in a heat exchanger tube. Parameters such as rod inclination angle, diameter ratio, and Reynolds number significantly influenced heat transfer and friction factor. Multi-objective optimization with artificial neural networks indicated that the 0.058-diameter and 57.057°-inclined vortex rod at 426767 Reynolds number provided the best heat transfer enhancement against pressure drop.

Li et al⁴⁷ explored the heat transfer and turbulent flow performance in a tube fitted with drainage inserts. They found that a 3.3 pitch ratio and a 45° inclination angle yielded the highest performance evaluation criterion, resulting in better heat transfer and flow performance.

Karagoz et al¹⁷ conducted experimental and numerical studies to enhance heat transfer rates using cylindrical turbulators in heat exchanger tubes. The effects of blade geometry and various turbulator configurations were explored. Experiments were performed with different turbulator ranges and angles, adjusting water flow rates to achieve the desired Reynolds numbers. The results revealed a significant increase in the Nusselt number due to the tube inserts, leading to energy savings. The study concluded that tube inserts significantly improve the Nusselt number, with the highest enhancement observed in the case of Sy1, which was 24% higher than in a straight tube. This research was also simulated using ANSYS Fluent 16 software to analyze flow behavior and heat transfer properties.

In the realm of horizontal components, 2-component gas–liquid slug flow is common in industrial applications, posing challenges for flow and heat transfer due to intermittent structures. The study aimed to estimate heat transfer properties for slug flow, developing a semi-theoretical heat transfer correlation based on Reynolds and Chilton–Colburn analogies. The research collected and analyzed 500 experimental data points and 8 heat transfer correlations, ultimately developing a new correlation.

This semi-theoretical correlation effectively estimated 91.5% of the data within a $\pm 30\%$ error margin. The study's applicability to other 2-phase flow regimes was also discussed.⁴⁸

Xin-Cheng et al⁴⁹ experimentally examined 2-phase flow distribution at the header of a single-plate heat exchanger, focusing on the liquification of natural gas with small liquid mass fractions. They used optical methods like Particle Image Velocimetry (PIV), Particle Tracking Velocimetry (PTV), and Laser-Induced Fluorescence (LIF) to measure liquid and gas flow rates. The research quantified and discussed the distribution of liquid and gas flows, specifically addressing the challenges and modifications required for porous deflectors or input nozzle configurations.

Karuppasamy et al⁵⁰ examined the turbulent forced convection of nanofluids in a circular tube with cone-shaped inserts. They used various nanofluid compositions and reported varying heat transfer enhancements. Different models were compared, with 2-phase mixture models proving more accurate.

Yadav and Sahu⁵¹ reported the impact of helical surface disc turbulators on heat transfer and pressure drop properties in a double-tube heat exchanger. They found that the lowest diameter ratio and increased helix angle led to higher Nusselt numbers and friction factors.

Xiong et al⁵² discussed the impact of conical and fusiform turbulators in a double-tube heat exchanger with circular inner tubes and varying configurations. They found that using a circular inner tube with a 12-mm fusiform turbulator resulted in the best thermal performance.

Mousa et al⁷ conducted a comprehensive review of single-phase heat transfer enhancement techniques. They classified methods into active and passive techniques, highlighting the advantages and challenges of each. Bashtani et al⁵³ numerically investigated the effects of adding aluminum oxide nanoparticles in a heat exchanger with turbulators. They found that turbulators significantly increased thermal effects, and the addition of nanofluid further improved heat transfer.

Khetib⁵⁴ conducted a numerical study to assess the effect of curved turbulators on the exergy efficiency of a solar collector using a 2-phase hybrid nanofluid. The study modeled the Multi-Wall Carbon NanoTubes (MWCNT)-TiO₂-water hybrid nanofluid and found that increasing Re and ϕ improved exergy efficiency. However, increasing the lateral ratio of the curved turbulators resulted in a decrease in exergy efficiency.

All the studies cited above focus on various methods and configurations to enhance heat transfer and reduce friction in heat exchangers and tubes, providing valuable insights for improving energy efficiency in different industries. Several methods, as well as modifications to turbulators or inserts, were investigated to achieve better heat transfer performance. Each study considered different parameters and geometries to optimize heat transfer and thermal efficiency.

Aim and Scope

Due to increased industrial needs and improved living standards, energy consumption has risen, making energy production more expensive. Therefore, there is a growing focus on researching, finding, and promoting alternative energy sources. Additionally, conserving and efficiently using energy has become a top priority worldwide. One crucial aspect of achieving energy efficiency and energy economy is enhancing heat transfer, which involves

the development of methods broadly categorized as "passive," "active," and "hybrid" methods.

In the context of 2-phase flows, the ideal state is characterized by stable flow, minimizing hydrodynamic and thermal fluctuations. Stable flow occurs when flow conditions within a channel change minimally, allowing the flow to asymptotically approach another stable state. In contrast, unstable flows do not asymptotically approach another state, exhibiting periodic oscillations in hydrodynamic and thermal properties such as flow rate, pressure, and temperature.

Unstable flows are common in 2-phase flow systems, such as cooling systems, steam generators, heat exchangers, steam boilers, and nuclear reactors. These flow instabilities, resulting from pressure and flow rate fluctuations, can lead to malfunctions and disruptions in the heat transfer components, significantly reducing the economic lifespan of these systems. Issues related to these fluctuations include thermal fatigue, boiling crises, mechanical vibrations, control difficulties due to transient high temperatures, and burn-out on the heat transfer surface, especially in nuclear power plant fuel elements.

Unstable 2-phase flows can manifest in various forms influenced by different factors and conditions. Understanding the mechanisms behind the formation of these instabilities is crucial for devising effective control and mitigation strategies. These instabilities are broadly classified into 2 categories: "static" and "dynamic" instabilities. Factors such as channel geometry, pressure, flow rate, and temperature play a significant role in influencing these instabilities.

Regarding steady-state characteristics, it was noticed that all improved surfaces exhibited a unique characteristic curve with a distinctive "S" shape. The onset of the 2-phase flow region typically occurred in the vicinity of the local minimum on this characteristic curve. Furthermore, there was a correlation between a decrease in inlet temperature and a subsequent reduction in pressure drop, with the pressure drops on the enhanced surfaces being consistently higher than those on conventional straight tubes.

In terms of stability boundaries, specific trends emerged. As the inlet temperature decreased, the point at which PDO (boundary of disturbance onset) occurred shifted toward lower mass flow rates. On improved surfaces, oscillations covered a broader section of the characteristic curve compared to their counterparts in straight tubes. The extent of this region was directly related to the duration of the oscillations. It is worth noting that the increased stability, particularly in cases where a helical spring element was used as an embedded enhancement device, may not be applicable universally to all improved surfaces.

Pressure drop oscillations revealed noteworthy patterns. As mass flow rates decreased, both the period and amplitude of PDO increased. Similarly, a reduction in the inlet temperature led to an upward trend in the period and amplitude of PDO. Furthermore, the improved surfaces consistently outperformed straight tubes in terms of both period and amplitude. The analysis extended to density fluctuation oscillations (DFO). It was observed that when mass flow rates decreased, the period and amplitude of DFO decreased as well. Conversely, a decrease in the inlet temperature resulted in an increase in the period and amplitude of DFO. Furthermore, improved surfaces consistently exhibited higher values for the period and amplitude of DFO when compared to

straight tubes. Lastly, the examination of thermal oscillations revealed consistent trends. Wall temperatures on improved surfaces consistently registered higher values than those seen in straight tubes. Moreover, the periods and amplitudes of these thermal oscillations were notably greater on improved surfaces. These thermal oscillations exhibited an increasing trend in both period and amplitude as the inlet temperature decreased and as mass flow rates decreased.

Given that experimental studies on 2-phase flow instabilities have predominantly focused on vertical tubes and channels, this thesis aims to investigate the impact of heat transfer improvements in horizontal tubes on 2-phase flow regimes and instabilities Table 1. To achieve this, experiments were conducted using a specially prepared test tube with an intermediate effective diameter. Various configurations with different pitch distances of helical wire inserts were used to assess their effects on flow stratification, amplitude, and oscillation periods.

This present study is aimed at contributing to scientific knowledge in the following ways:

- Designing 2-phase flow evaporators and heat exchangers with consideration of potential instabilities, preventing burnout, thermal fatigue, vibrations, and malfunctions, is important. The burnout phenomenon is influenced by geometry, operational conditions, and boundary conditions, such as axial heat flux distribution.
- Determining the effects and consequences of 2-phase flow instabilities on tube effective diameters and exploring the boundaries of oscillations and flow patterns.
- Despite the existing body of literature on 2-phase flow instabilities, research on the impact of heat transfer enhancement on these instabilities is limited. Therefore, this study, coupled with subsequent numerical modeling, is expected to make a significant contribution to this field.

MATERIAL AND METHODS

Experimental Setup

The experiments were conducted within the heat transfer laboratory of the Mechanical Engineering Department, utilizing a horizontal tubular test system. This setup was configured to obtain 2-phase flow and facilitate the investigation of pressure

Table 1. Effect of Heat Transfer Improvement on 2-Phase Flow Instabilities⁵⁵

Parameters	Characteristics
Steady state characteristics	<ol style="list-style-type: none"> 1. The characteristic curve on all treated surfaces is slanted S-shaped. 2. The 2-phase flow region starts around the local minimum of the characteristic curve. 3. As the inlet temperature decreases on improved surfaces, the pressure drop decreases. 4. Pressure drops on improved surfaces are higher than in straight Tubes.
Stability limits	<ol style="list-style-type: none"> 1. As the inlet temperature decreases, the starting point of PDO shifts to a lower flow rate. 2. With improved surfaces, oscillations cover a larger region in the characteristic curve than in a plain Tube. The larger this region, the longer the oscillations last. 3. When using a spring element as a built-in recovery device, stability increases as the effective diameter decreases. However, this result cannot be generalized to other improved surfaces.
Pressure drop oscillations	<ol style="list-style-type: none"> 1. As the mass flow rate decreases, the period and amplitudes of the PDO increase. 2. As the inlet temperature decreases, the periods and amplitudes of the PDO increase. 3. The periods and amplitudes of PDO with improved surfaces are higher than those in plain tube.
Density change oscillations	<ol style="list-style-type: none"> 1. As the mass flow rate decreases, the period and amplitudes of the DFOs decrease. 2. As the inlet temperature decreases, the periods and amplitudes of the DFO increase. 3. The periods and amplitudes of DFO with improved surfaces are higher than those in plain tubes.
Thermal oscillations	<ol style="list-style-type: none"> 1. Wall temperatures of improved surfaces are higher than those of straight Tubes. 2. The periods and amplitudes of wall temperatures with improved surfaces are higher than those in plain tubes. 3. The periods and amplitudes of thermal oscillations increase with decreasing inlet temperature. 4. The periods and amplitudes of thermal oscillations increase with decreasing mass flow rate.

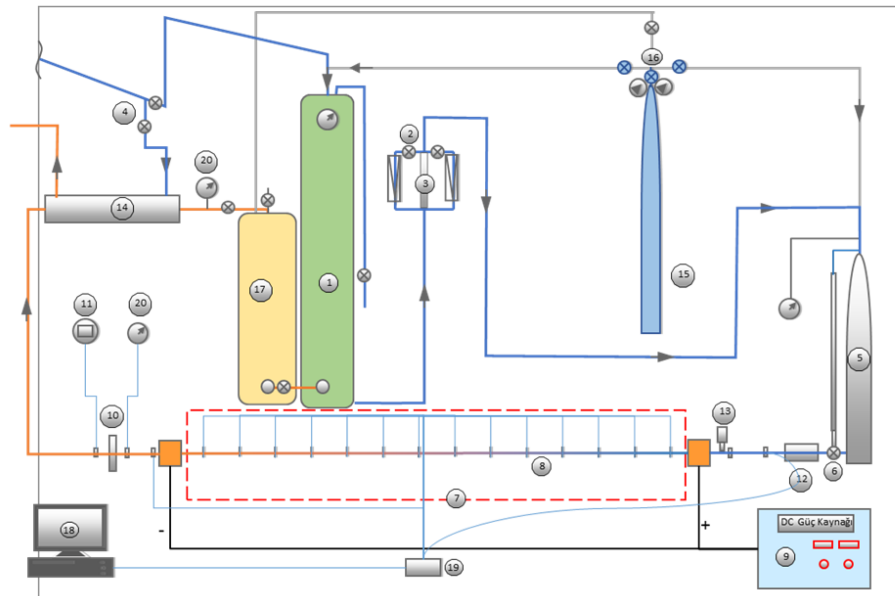
drop-type oscillations, density change-type oscillations, and thermal oscillations. The study focused on the effects of heat flux, flow rate, and tube internal elements consisting of differently stepped tapered coil arrays on the 2-phase stable and unstable flow characteristics in horizontal tubes.

As illustrated in Figure 1, the experimental setup consists of 3 main sections: fluid supply, test section, and storage section.

Fluid Supply Section

The fluid supply section, responsible for delivering water under specified conditions to the test tube, includes the main supply





Fluid Supply Section	Test Section	Fluid Discharge Section
1- Main supply tank	8- Test tube	15- Nitrogen tank
2- Flow rate arrangement valve	9- DC power supply	16- Regulator
3- Flowmeter (2 pcs)	10- Orifice	17- Storage tank
4- Valve	11- Digital manometer	18- Computer
5- Balancing tank	12- Flow transducer	19- Data acquisition card
6- Inlet control valve	13- Pressure transducer	20- Needle manometer
7- Test chamber	14- Condenser	

Figure 1. Photographic and schematic views of the experimental setup.

tank, a flow control valve, 2 flowmeters (one with a 0–400 L/h range and the other with a 0–1000 L/h range), a digital flow transducer, and a nitrogen tank with a pressure regulator.

The cylindrical main supply tank, which has a volume of 0.7 m³ and stands vertically at a height of 3 meters, is designed to store the required water for the duration of the experiment. It is capable of withstanding an operating pressure of up to 50 bar (Figure 1). The flow rate of the fluid in the supply line is controlled using a control valve. Two flowmeters and a digital flow transducer are employed to measure and adjust the flow rate. These flowmeters have a maximum operating pressure of 40 bar and a maximum operating temperature of 100°C, all of which are constructed from steel.

Test Section

The test section is the primary area of interest in the study where the targeted parameters are effective. It comprises nine elements, including a balance tank (5), an inlet flow control valve (6), a test chamber (7), a test tube (8), a DC power supply (9), an orifice (10), a digital manometer (11), turbine-type flow meters (12), and a pressure transducer (13).

In the event that the test tube's length is insufficient, a balance tank with a volume of 0.05 m³ is utilized to create a compressible volume. Additionally, to observe variations in fluid levels and compressible volume levels, a transparent plastic level gauge and a pressure gauge capable of withstanding 30 bars are connected to the balance tank, as depicted in Figure 1.

Between the balance tank and the test tube, components such as a turbine-type flow meter, Bourdon-type manometer, pressure transducer, and temperature measurement device are installed, as shown in Figure 1. A turbine-type flow meter is used to measure fluctuations in fluid flow; the Bourdon-type manometer measures fluid pressure at the test tube's inlet; and the pressure transducer is employed to measure fluctuations in fluid pressure at the inlet of the test tube. The fluid's inlet temperature is measured using a T-type thermocouple, and experiments are conducted within a mass flow rate range of 22 to 80 g/s.

A DC power supply with an approximate power rating of 40 kW is connected to the test chamber's inlet and outlet sections via its positive and negative terminals to transfer thermal power to the test tube. The heat power values supplied to the test tube are read from the digital voltage and current indicators on the DC power supply (Figure 2).

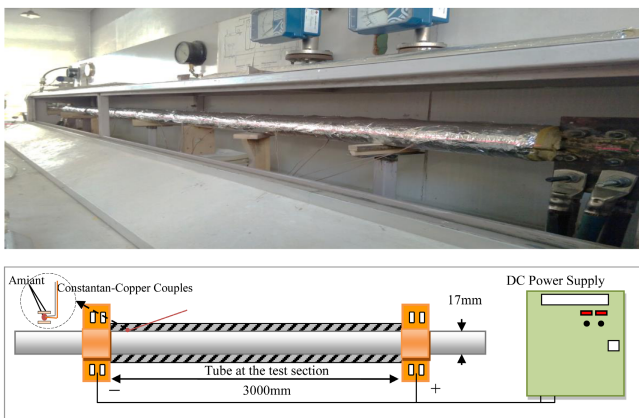


Figure 2. Test section with connections and instruments.

To achieve the desired pressure drop and determine the effects of the outlet restrictor on flow oscillations, an orifice plate is attached at the test tube's outlet, as shown in Figure 1. The pressure at the inlet side of the orifice plate is measured using a Bourdon-type manometer, and the pressure at the outlet side is measured using a Bourdon-type digital manometer.

Fluid Storage Section

The fluid storage section is composed of 2 primary elements: the condenser (14) and the fluid storage tank (17). This section is where the fluid is directed after leaving the test section. Typically, the fluid exits the test tube in a vapor phase and is then condensed in a water-cooled condenser to return it to its starting conditions. The condensed fluid is subsequently pumped into the storage tank. When needed, it can be pressurized using high-pressure nitrogen gas and fed back into the main supply tank or discharged.

The condenser, a horizontal body-tube heat exchanger, is employed to convert the fluid from the vapor phase to the liquid phase. The condenser body is constructed from a seamless black tube with a diameter of 0.16 m and a length of 1.45 m. Inside it, a 0.02-m-diameter copper tube is spirally placed, allowing the fluid from the test section to pass through from the outside while cooling water flows through the inside.

In the condenser, the fluid undergoes a phase change and is then sent to a vertical storage tank with a diameter of 0.75 m, a height of 1.75 m, and a wall thickness of 1 cm. From this storage tank, the fluid is pressurized using high-pressure nitrogen gas and pumped into the main supply tank when needed, or it can be discharged by opening the relief valve.

Uncertainty Analysis

Uncertainty analysis is a crucial aspect of any experimental study, as it quantifies the reliability and precision of measurements. Understanding and evaluating the uncertainty in measurements is essential for drawing meaningful conclusions and ensuring the validity of experimental results.

The experimental measurements were conducted in various aspects, including temperature, pressure, flow rate, and heat power. Each of these measurements was taken with a certain degree of precision, and their relative uncertainties were assessed (Table 2). Here is a reorganized summary of the measurements and their associated uncertainty:

Temperature Measurements

- Temperature measurements were made at 30 points along the experimental system using T-type copper-constantan thermocouples with a 0.25 mm diameter.
- A precision of $\pm 0.5^\circ\text{C}$ was achieved in these temperature measurements.
- In the test tube, temperature readings were taken using thermocouples attached to the tube wall, placed between 2 asbestos plates.
- At the inlet and outlet of the test tube, temperature measurements were carried out with thermocouples placed inside 5-mm-diameter closed-ended copper tubes.
- A total of 28 T-type thermocouples were installed along the length of the test tube at equal intervals (as shown in Figure 1).
- To minimize electrical interference and reduce noise, the thermocouple junctions were electrically insulated but had good thermal conductivity between the asbestos plates.

Table 2. Uncertainties in measurements

Measurement Type	Relative Uncertainty
Temperature	0.1°C to 0.5°C
Pressure	0.1%
Flow rate	0.4%
Heat power	0.2%

- Data was collected using an analog/digital Advantech Data Acquisition card and VisiDAQ 3.1 software.
- The total error in temperature measurements ranged from 0.1°C to 0.5°C, depending on the selected gain value of the control card.

Pressure Measurements

- Pressure measurements were conducted at several points in the system, including the main tank, balance tank, nitrogen tank, and before and after the orifice.
- Bourdon-type analog manometers with a precision of ± 0.1 bar were used to measure pressure in the main tank, balance tank, nitrogen tank, and the inlet of the orifice.
- The pressure after the orifice was measured using a digital manometer with a 0.5 bar resolution.
- The analog signals from the Bourdon-type manometers and pressure transducers were processed using a data acquisition card (as seen in Figure 1).
- The total error in the pressure measurements was 0.1%.

Flow Rate Measurements

- Precise mass flow rate measurements were essential for determining the oscillation limits and stability boundaries of flow regimes.
- Flow rate adjustment was facilitated by a control valve in the system.
- Two flowmeters were used to measure and adjust the flow rate, with a total error of 0.4%. These flowmeters had measurement ranges of 0-400 L/h and 0-1000 L/h.
- Experiments were conducted within a mass flow rate range of 25 to 140 g/s.
- A turbine-type flow meter was installed between the balance tank and the test tube to measure flow rate oscillations.
- The total error in flow rate measurements was 0.05%.

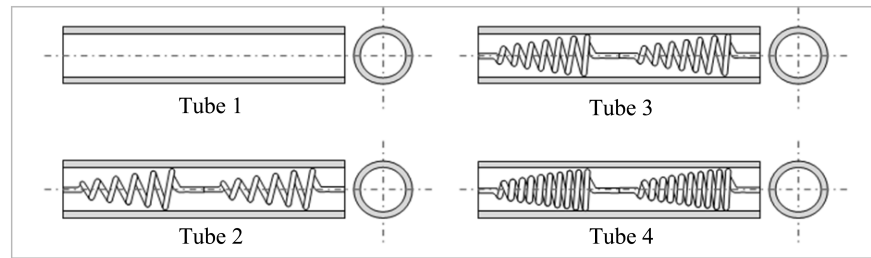
Heat Power Measurements

- Approximately 40 kW of DC power supply was used in the experimental setup.
- The voltage and current values could be adjusted and read independently on the power supply.
- The total error in electrical power measurements was determined to be 0.2%.

Experimental Method

Experimental studies were carried out in 2 stages: stable experiments, in which steady-state characteristics were determined, and unstable experiments, in which 2-phase flow dynamic instabilities were investigated. The experiments were carried out at constant thermal power, constant fluid inlet temperature, constant outlet orifice diameter, and 4 different types of tubes.

The heat transfer surfaces and characteristics of the heat transfer improvement elements whose photographs are shown in Figure 4 are given in Figure 3. The plain tube without a surface-increasing element is named tube 1, and the tubes with surface-increasing elements consisting of conical wound spring arrays with different spring steps are named tube 2, tube 3, and tube 4. As shown in



Name	Specifications	De (mm)
Tube-1	Plain Tube (no inserts)	17.60
Tube-2	1.8mm wire diameter, 150mm spacing, 30mm pitched conical spring array	17.48
Tube-3	1.8mm wire diameter, 150mm spacing, 20mm pitched conical spring array	17.45
Tube-4	1.8mm wire diameter, 150mm spacing, 10mm pitched conical spring array	17.34

Figure 3. Insert configurations and their specifications.

Figure 3, heat transfer surfaces are characterized by the effective diameter calculated using the following equation:

$$d_e = \sqrt{\frac{4V'}{\pi L}} \quad (1)$$

where V' is the internal volume and L is the length of the tube.

Experiments were conducted to determine steady-state characteristics, starting with a plain tube and a constant outlet orifice restriction. These experiments were performed at an inlet temperature (T_i) of 20°C and a heat power (Q) of 22 kW. Subsequently, unstable experiments were conducted under the same experimental parameters. The tests included tube 1, followed by tube 2, tube 3, and tube 4.

The following parameters were measured for each experiment:

- Surface temperatures of the test tube (14 readings at the bottom and 14 at the top, totaling 28 readings).
- Inlet and outlet temperatures of the fluid in the test tube.
- Static pressure at the inlet and outlet of the test tube.
- Inlet mass flow rate of the test tube.
- Mass flow rate oscillations at the inlet of the test tube.
- Pressure oscillations at the inlet of the test tube.
- Pressure at the inlet and outlet of the orifice.

Steady-state characteristic experiments aim to determine the pressure drop as a function of mass flow rate and are represented graphically. This pressure drop is the difference between

the equilibrium tank pressure and the fluid pressure after the orifice plate. The experiments commenced with a mass flow rate (\dot{m}) of 80 g/s and were then reduced at intervals of approximately 8-10 g/s to establish the characteristic curve. To fully understand the characteristics of steam flow, the mass flow rate was reduced to very low values. The lowest mass flow rate was set at 22 g/s due to burnout concerns. Observations of wall temperatures and fluid outlet temperatures were made to detect burnout conditions.

The experimental process to determine steady-state characteristics followed these steps:

- The main tank was pressurized to the system pressure using nitrogen gas, adjusting the system pressure with a pressure regulator valve on the nitrogen cylinder.
- To ensure that there was no compressible volume in the unused balancing tank during steady-state experiments, the nitrogen gas inside the balancing tank was vented by monitoring the level indicator.
- The mass flow rate was adjusted to the maximum value determined in the experimental work by using a control valve.
- The digital thermostat was used to set the inlet temperature of the water from the main tank to the test tube.
- The cooling water circuit of the heat exchanger condensing the working fluid was activated.
- The system was started, and stability was awaited.
- An adjustable DC power supply was used to apply heat to the system, ensuring that the required heat power was attained.

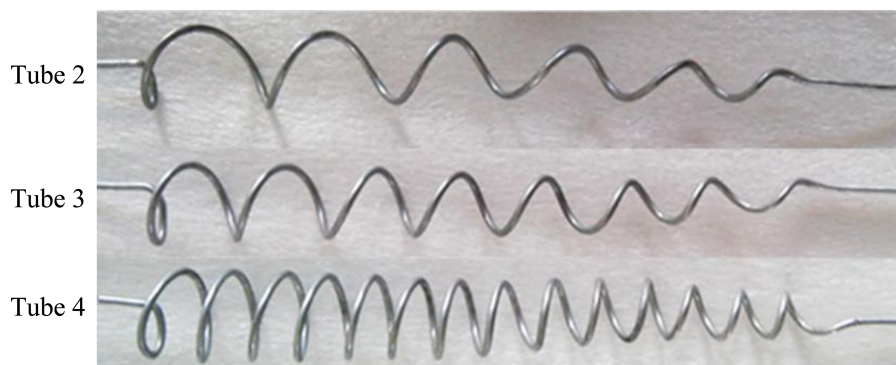


Figure 4. Conical spring inserts used in each tube for heat transfer enhancement.

- The system was allowed to reach a stable state, as confirmed by no more than a 0.5°C variation in test tube surface temperatures. When this stability was achieved, measurements were taken, and the experiment for the given mass flow rate was considered complete.
- The above steps were repeated for different mass flow rates until the inlet mass flow rate reached 22 g/s.

Unstable state characteristic experiments aimed to investigate dynamic flow instabilities, including pressure drop type, density fluctuation type, and thermal oscillations. To induce instabilities, a compressible volume was ensured in the balancing tank before the test section. The water level inside the balancing tank was maintained at a specific level using a constant gas pressure obtained from the nitrogen tank. While the compressible volume was held constant in all experiments, the magnitude of this volume varied due to oscillations in mass flow and pressure.

The steps for conducting unstable-state experiments were as follows:

- The system was pressurized with nitrogen gas from the nitrogen tank, adjusting the system pressure with a regulator.
- To allow comparisons based on the presence of a compressible volume in the balancing tank, the balancing tank was pressurized in all experiments using a pressurized nitrogen tank and regulator, and the water level in the transparent level indicator was adjusted.
- The mass flow rate was adjusted to achieve the maximum flow rate determined in the experimental work.
- The cooling water circuit of the heat exchanger was activated.
- The system was started and verified for weak yet stable operation.
- Thermal power was transferred to the system by adjusting the current and voltage through the DC power supply.
- Instantaneous temperature values were monitored via thermocouples, and the system was allowed to stabilize, as indicated by temperature changes not exceeding 0.5°C.
- Experiments continued with a gradual reduction in mass flow rate until the point of oscillation onset.
- To determine the transition from boiling-dominated oscillations (PDO) to independent vapor-dominant oscillations (DFO), small reductions in mass flow rate were made, and low oscillation periods were examined.

- Wall temperatures and flow temperatures were observed carefully as mass flow decreased, especially concerning thermal oscillations.
- When significant deviations between wall and fluid temperatures indicating the onset of burnout were observed, the heat power was cut, and the experimental work was terminated.

RESULTS AND DISCUSSION

Stable state characteristic curves, represented by an x - y plot of pressure drop versus mass flow rate, commonly used to understand flow characteristics in 2-phase flow systems, were created for each test tube, and pressure drop values were calculated using the difference between the equilibrium tank pressure and the test tube outlet pressure at various mass flow rates. The curves exhibit positively sloped sections corresponding to high mass flow rates in the single-phase liquid region, where the minimum occurs. The negatively sloped region indicates the inception of 2-phase flow with the formation of initial bubbles. As the number of bubbles increases, both the liquid and vapor phases coexist, leading to a lower fluid density compared to the liquid phase, consequently causing an increase in pressure drop. Further reduction in mass flow rates leads to the transition from the negatively sloped region to the positively sloped one as the pressure drop values decrease.

Comparison of Stable-State Curves

Characteristic state curves were generated for each test tube, comparing their values for parameter 'k'. The experiments were conducted with a constant inlet fluid temperature ($T_i=20^\circ\text{C}$) and a constant heat power ($Q=22\text{ kW}$), including measurements without power input ($Q=0$). Figure 6, 7 and 8 illustrate the temperatures of the lower and upper tube walls at no power and power conditions. The characteristic state curves are provided for each tube. A comparison of pressure drop values reveals differences among the 4 test tubes. Tube 4, equipped with surface enhancement elements composed of 10 mm pitch springs, exhibited the highest pressure drop value, whereas tube 1 had the lowest pressure drop value. When ranked based on pressure drop values, the tubes were observed to have ranked as tube 1 < tube 2 < tube 3 < tube 4. In tubes with surface enhancement elements, flow stratification and frictional pressure drops caused an even bigger drop in pressure. This was because the vapor phase caused more pressure drop as the mass flow rates dropped, which was higher than the pressure drop values in plain tubes. Increased system

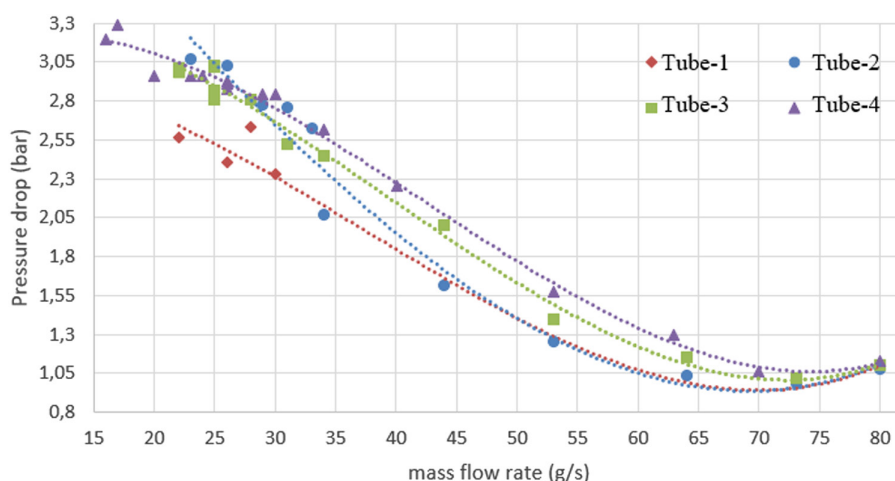


Figure 5. Pressure drop in the tubes at different mass flow rates.

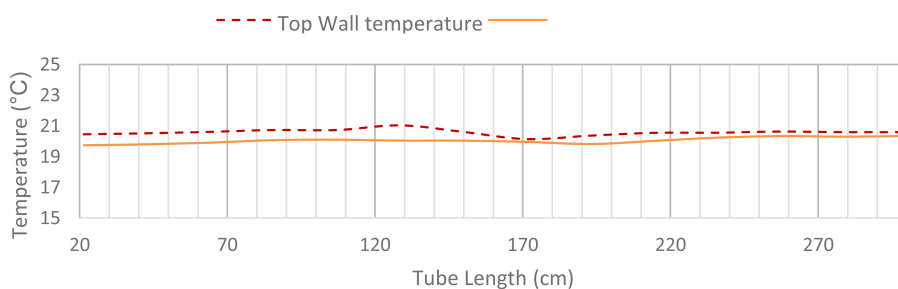


Figure 6. Top and bottom wall temperatures with tube 1 at no-power condition.

instability is associated with regions in the stable state curves where the negative slope angle becomes steeper. In such cases, plain tube curves are expected to have fewer negative slope regions compared to the curves of tubes with surface improvement elements, and the graphs confirm this expectation.

This analysis reveals how the addition of surface enhancement elements in tubes affects stable state characteristics and pressure drop values, with tube 1 having the lowest pressure drop and tube 4 the highest.

As a result of the experiments that continued by reducing the mass flow by small amounts, $m=28$ g/s, $m=26$ g/s, and $m=22$ g/s were determined as the comparison criteria of the in-Tube elements, and how each element would change this curve with the same system parameters was examined.

When all tubes are examined in themselves, it is seen that there is an increase in both lower and upper wall temperatures as the mass flow decreases. When sorted in terms of whether there is a significant separation between the lower (Figure 10) and upper

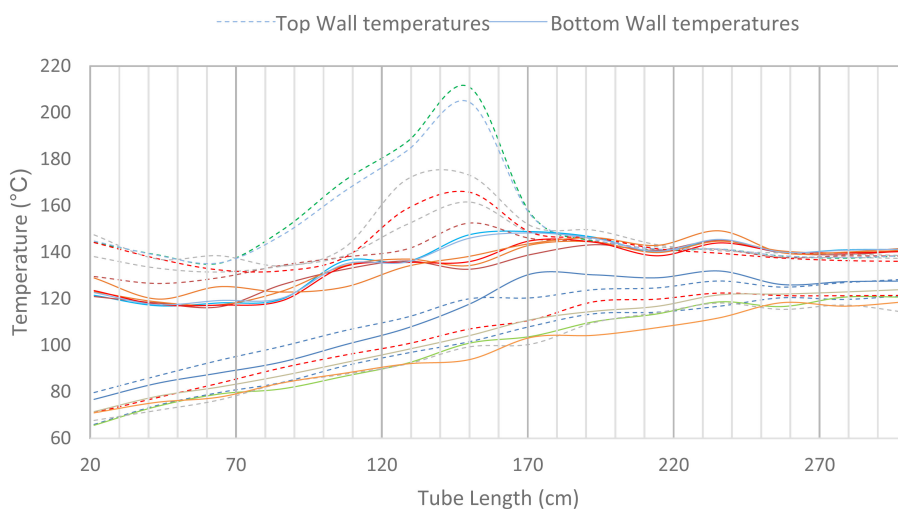


Figure 7. Top (- -) and bottom (—) Wall temperatures for all mass flow rates tested with tube 1.

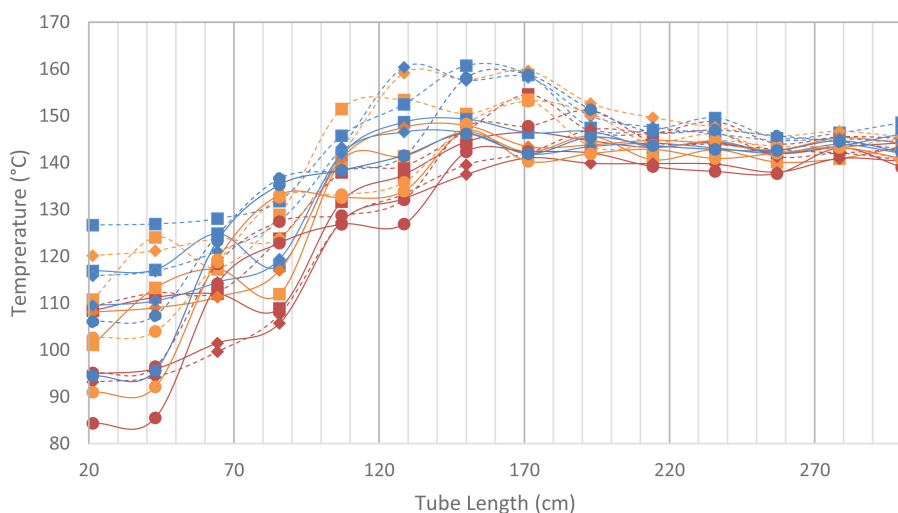


Figure 8. Top (- -) and bottom (—) Wall temperatures at 22 (blue), 26 (orange), and 28 (red) g/s mass flow rates in tube 2 (■), tube 3 (◆), and tube 4 (●).

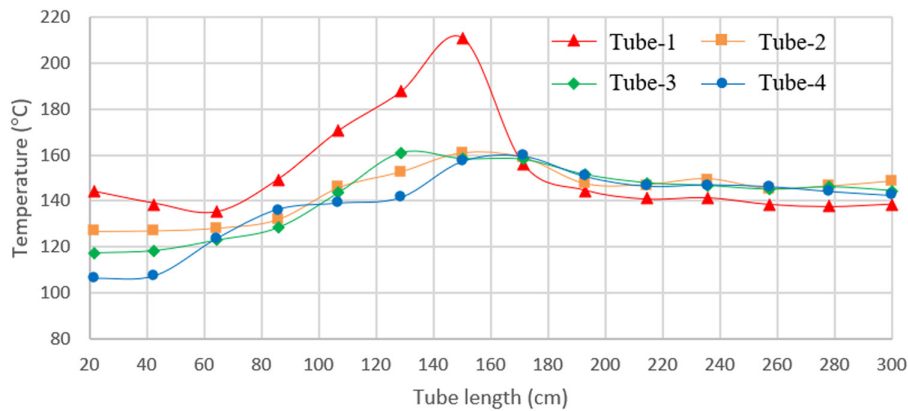


Figure 9. Top Wall temperatures at $\dot{m} = 22$ g/s in all tubes.

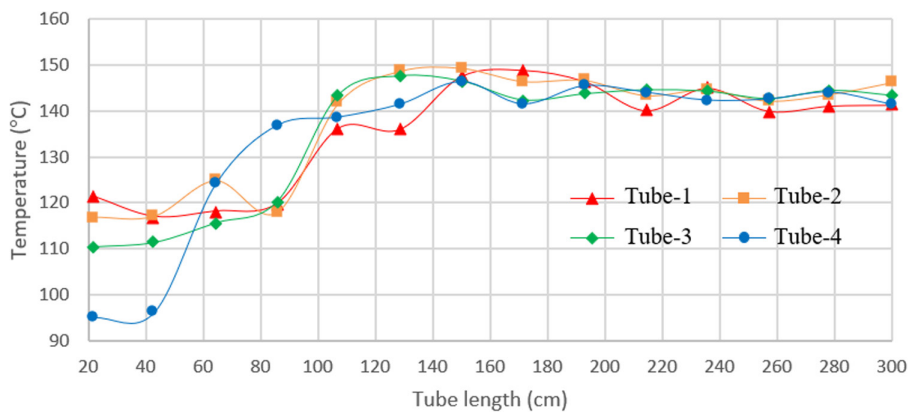


Figure 10. Bottom wall temperatures at $\dot{m} = 22$ g/s in all tubes.

(Figure 9) wall temperatures, it is seen that the most significant separation occurred at a flow rate of 22 g/s for tube 1, followed by tube 2, tube 3, and tube 4, respectively.

Although the tube diameter, wall thickness, inlet water temperature, and thermal power used in this study are unique in combination, the results obtained are consistent with the literature in terms of ensuring interphase coalescence and interaction, especially in 2-phase flow systems with stratified flow and circular flow regimes.

In this study, 2-phase flow events in forced-convection horizontal tubes were experimentally examined. The effects of heat transfer surface enhancement elements on stable and unstable flow events were investigated. Four different tubes were employed in the study: one was a plain tube, and the other 3 had surface enhancement elements consisting of helical springs with equal pitch and conicity angles, with 10 mm, 20 mm, and 30 mm pitch increments. The experiments were conducted in a 2-phase flow system with water as the working fluid under constant thermal power, outlet orifice diameter, fluid inlet temperature, and inlet pressure conditions. The experimental results can be summarized as follows:

- Characteristic curves for each tube exhibited differences in pressure drop values, indicating that the use of internal elements increased the pressure drop.
- Experiments were conducted at different mass flow rates while keeping thermal power, system pressure, fluid inlet temperature, outlet restrictor, and compressible volume constant.

The goal of this study was to find out how heat transfer and pressure drop are affected by helical spring arrays that are used as inserts in a forced-convection, boiling, horizontal, 2-phase flow tube system. For future research, the following recommendations can be made:

- The performance and effects of tube internal elements, including bent, strip, helical, and spring-like structures, should be compared under identical experimental conditions to evaluate their performance in the same experimental system.
- Geometric parameters of tube internal elements, such as the distance between each spring array, the conicity angle of springs, and the orientation of conical springs in the flow direction, should be examined and compared with the results of this study to fully determine their effects.
- An investigation of the orientation of helical springs in relation to flow instability, oscillation boundaries, and heat transfer effects should be conducted.
- Altering the distances and winding lengths of helical spring arrays with equal intervals and comparing the effects of these parameters.
- The experimental results of this entirely experimental study can be analyzed numerically and compared with experimental data to assess the consistency of the numerical and experimental results.
- The applicability of helical spring arrays in vertical or inclined systems can be compared with the findings of this study, considering the study was conducted in a horizontal tube system.

- Research can be carried out by changing parameters such as the size of the natural compressible volume, the heat transfer method, and the tube diameter in the construction and operation of the test system.
- To achieve more homogeneous energy distribution to the test tube, a different method can be employed, different from the way the heat energy was applied to the tube, which was connected to the near ends of the inlet and outlet. This change in energy application is needed to reduce uncertainties in wall temperature measurements.

Peer-review: Externally peer-reviewed.

Author Contributions: Concept – Ö.Ç.; Design – Ö.Ç., M.K.Y.; Supervision – Ö.Ç.; Resources – Ö.Ç., M.K.Y.; Materials – Ö.Ç., M.K.Y.; Data Collection and/or Processing – M.K.Y.; Analysis and/or Interpretation – M.K.Y.; Literature Search – Ö.Ç., M.K.Y.; Writing Manuscript – M.K.Y.; Critical Review – Ö.Ç., M.K.Y.

Declaration of Interests: The authors declare that they have no competing interest.

Funding: The authors declared that this study has received no financial support.

REFERENCES

- Godino DM, Corzo SF, Ramajo DE. Two-phase modeling of water-air flow of dispersed and segregated flows. *Ann Nucl Energy*. 2020;149:107766. [CrossRef]
- Wang W, Yang D, Liang Z, Qu M, Ouyang S. Experimental investigation on flow instabilities of ultra-supercritical water in parallel channels. *Applied Therm Engineering*. 2019;147:819-828. [CrossRef]
- Yeoh G. *Handbook of Multiphase Flow Science and Technology*; 2020. [CrossRef]
- Kakaç, S., A Review of Two-Phase Flow Instabilities. In *Advances in Two-Phase Flow on Heat Transfer*, Martinus, Nijhoff, Boston, vol.11, 577-668,1994.
- Bergles AE. *Review of Instabilities in Two Phase Systems. Two Phase Flows and Heat Transfer* (Kakaç S, Mayinger F, eds, vol 1). 1977:383-385.
- Cao Z, Wu Z, Luan H, Sunden B. Numerical study on heat transfer enhancement for laminar flow in a tube with mesh conical frustum inserts. *Numer Heat Transf A*. 2017;72(1):21-39. [CrossRef]
- Mousa MH, Miljkovic N, Nawaz K. Review of heat transfer enhancement techniques for single phase flows. *Renew Sustain Energy Rev*. 2021;137:110566. [CrossRef]
- Liu H, Zheng G, Man C, Jiang K, Lv X. Numerical and experimental studies on heat transfer enhancement in a circular tube inserted with twisted tape inserts. *Am J Energy Eng*. 2021;9(2):30. [CrossRef]
- Shivamallaiiah MM, Fernandes DV. Numerical investigation of heat transfer and friction factor characteristics of circular tube fitted with an array of semi-elliptical vortex generator inserts. *Cogent Eng*. 2021;8(1). [CrossRef]
- Nikoozadeh A, Behzadmehr A, Payan S. Numerical investigation of turbulent heat transfer enhancement using combined propeller-type turbulator and nanofluid in a circular tube. *J Therm Anal Calorim*. 2020;140(3):1029-1044. [CrossRef]
- Mohammed HA, Ali Abuobeida IAM, Vuthaluru HB, Liu S. Two-phase forced convection of nanofluids flow in circular tubes using convergent and divergent conical rings inserts. *Int Commun Heat Mass Transf*. 2019;101:10-20. [CrossRef]
- Chamolli S, Lu R, Xie J, Yu P. Numerical study on flow structure and heat transfer in a circular tube integrated with novel anchor shaped inserts. *Applied Therm Engineering*. 2018;135:304-324. [CrossRef]
- Liu P, Zheng N, Shan F, Liu Z, Liu W. An experimental and numerical study on the laminar heat transfer and flow characteristics of a circular tube fitted with multiple conical strips inserts. *International J Heat Mass Transf*. 2018;117:691-709. [CrossRef]
- Waghole DR. Experimental and numerical investigation on heat transfer augmentation in a circular tube under forced convection with annular differential blockages/inserts. *Heat Mass Transfer*. 2018;54(6):1841-1846. [CrossRef]
- Jinxing W, Chao W, Mingqiang W, Yanhui L, Yafei L. Numerical Simulation of Turbulent Fluid Flow and Heat Transfer in a Circular Tube with Twisted Tape Inserts. *Journal of Zhengzhou University (Engineering Science)* (2017) 38(02):10-14.
- Jassim NA, Abdul Hussin K, Abdul Abbass NY. Numerical investigation of heat transfer enhancement in circular tube using twisted tape inserts and nanotechnology. *Wasit J Eng Sci*. 2017;5(2):42-54. [CrossRef]
- Karagoz S, Afshari F, Yildirim O, Comakli O. Experimental and numerical investigation of the cylindrical blade tube inserts effect on the heat transfer enhancement in the horizontal pipe exchangers. *Heat Mass Transfer*. 2017;53(9):2769-2784. [CrossRef]
- Zheng N, Liu P, Wang X, Shan F, Liu Z, Liu W. Numerical simulation and optimization of heat transfer enhancement in a heat exchanger tube fitted with vortex rod inserts. *Appl Therm Eng*. 2017;123:471-484. [CrossRef]
- Raheemah SH, Ashham MA, Salman K. Numerical investigation on enhancement of heat transfer using rod inserts in single pipe heat exchanger. *J Mech Eng Sci*. 2019;13(4):6112-6124. [CrossRef]
- Adiguzel N, Göcücü A. Experimental investigation of the effects of ring turbulators on heat transfer in two-phase flow. *Iran J Sci Technol Trans Mech Eng*. 2021:1-10. [CrossRef]
- Anvari AR, Javaherdeh K, Emami-Meibodi M, Rashidi AM. Numerical and experimental investigation of heat transfer behavior in a round tube with the special conical ring inserts. *Energy Convers Manag*. 2014;88:214-217. [CrossRef]
- Outokesh M, Ajarostaghi SSM, Bozorgzadeh A, Sedighi K. Numerical evaluation of the effect of utilizing twisted tape with curved profile as a turbulator on heat transfer enhancement in a pipe. *J Therm Anal Calorim*. 2020;140(3):1537-1553. [CrossRef]
- Mashayekhi R, Arasteh H, Toghraie D, Motaharpour SH, Keshmiri A, Afrand M. Heat transfer enhancement of water- Al_2O_3 nanofluid in an oval channel equipped with two rows of twisted conical strip inserts in various directions: a two-phase approach. *Comput Math Appl*. 2020;79(8):2203-2215. [CrossRef]
- Agrebi S, Solano JP, Snoussi A, ben Brahim A. Numerical simulation of convective heat transfer in tube with wire coil inserts. In: 2015 World Symposium on Mechatronics Engineering & Applied Physics (WSMEAP): IEEE; 2015. [CrossRef]
- Abbas EF, Weis MM, Ridha AS. Experimental and numerical study of heat transfer enhancement in a shell and tube heat exchanger using helical coiled wire inserts. *Tikrit J Eng Sci*. 2018;25(2):74-79. [CrossRef]
- Min C, Li H, Gao X, Wang K, Xie L. Numerical investigation of convective heat transfer enhancement by a combination of vortex generator and in-tube inserts. *Int Commun Heat Mass Transf*. 2021;127:105490. [CrossRef]
- Davidov AA. *Elimination of Pulsation in Once through Boilers*, vol 3. USSR: Elektricheskije Stantzu, 1956:36-43.
- Stenning AH, Veziroğlu TN. Flow oscillation modes in forced convection boiling. In: *Proc. Heat Transfer and Fluid Mechanics Institute*. Palo Alto: Stanford Univ. Press; 1965:301-316.
- Veziroğlu TN, Lee SS. Boiling upward flow instabilities. AEC- Oak Ridge National Laboratory Subcontract. 1968;2975.
- Veziroğlu TN; Lee, SS, Boiling flow instabilities in a two parallel channel upflow system, Final Report to AEC-Oak Ridge National Laboratory Subcontract No. 2975, 1969.
- Veziroğlu, TN and Lee, SS. Instabilities in boiling upward flow. In *Proceedings of International Symposium On Concurrent Gas-Liquid Flow*. 1968.

32. Aritomi M, Aoki S, Inoue A. Instabilities in parallel channel of forced convection boiling upflow system. *J Nucl Sci Technol*. 1977;1-30.
33. Aritomi M, Aoki S, Inoue A. Instabilities in parallel channel of forced convection boiling upflow system (V). *J Nucl Sci Technol*. 1982;20(4):286-301.
34. Aritomi M, Aoki S, Inoue A. Instabilities in parallel channel of forced convection boiling upflow system (II). *J Nuc Sci Tech*. 1979;14(2):88-96.
35. Kakaç S, Veziroğlu TN, Padki MM, Fu LQ, Chen XJ. Investigation of thermal instabilities in a forced convection upward boiling system. *Exp Therm Fluid Sci*. 1990;3(2):191-201. [\[CrossRef\]](#)
36. Padki MM, Palmer K, Kakaç S, Veziroğlu TN. Bifurcation analysis of pressure drop oscillations and the Ledinegg instability. *Int J Heat Mass Transf*. 1992;35(2):525-532. [\[CrossRef\]](#)
37. Ding Y. *Experimental Investigation of Two Phase Flow Phenomena in Horizontal Convective in Tube Boiling System* (Ph.D. Thesis). Florida USA: University of Miami; 1993:21-65.
38. Xiao M, Chen XJ, Zhang MY, Veziroğlu TN, Kakaç S. A multivariable linear investigation of two phase flow instabilities in parallel boiling channels under high pressure. *Int J Multiphase Flow*. 1993;19(1):65-77. [\[CrossRef\]](#)
39. Liu HT, Kakaç S, Mayinger F. Characteristics of transition boiling and thermal oscillation in an upflow convective boiling system. *Exp Therm Fluid Sci*. 1994;8(3):195-205. [\[CrossRef\]](#)
40. Liu HT, Kakaç S, Mayinger F. Characteristics of transition boiling and thermal oscillations in an up flow convective boiling system. In: 29th ASME/ AIChE/ ANS/ AIAA, National Heat Transfer Conference. Atlanta, Georgia; 1993:8-11.
41. Guo L-J, Feng Z-P, Chen X-J. Pressure drop oscillation of steam-water two-phase flow in a helically coiled tube. *Int J Heat Mass Transf*. 2001;44(8):1555-1564. [\[CrossRef\]](#)
42. Çomaklı Ö, Karslı S, Yılmaz M. Experimental investigation of two phase flow instabilities in A horizontal in-tube boiling system. *Energy Convers Manag*. 2002;43(2):249-268. [\[CrossRef\]](#)
43. Yu W, France DM, Wambsganss MW, Hull JR. Two-phase pressure drop, boiling heat transfer, and critical heat flux to water in a small-diameter horizontal tube. *Int J Multiphase Flow*. 2002;28(6):927-941. [\[CrossRef\]](#)
44. Salman SD, Kadhum AAH, Takriff MS, Mohamad AB. Numerical investigation of heat transfer and friction factor characteristics in a circular tube fitted with V-cut twisted tape inserts. *ScientificWorldJournal*. 2013;2013:492762. [\[CrossRef\]](#)
45. Alam T, Saini RP, Saini JS. Heat and flow characteristics of air heater ducts provided with turbulators—A review. *Renewable and Sustainable Energy Reviews* (2014) 31:289–304. doi:[\[CrossRef\]](#)
45. Razzaghi H, Layeghi M, Goodarzi S, Lotfizadeh H. Numerical analysis of the effects of changeable transverse and longitudinal pitches and porous media inserts on heat transfer from an elliptic tube bundle. *Journal of Theoretical and Applied Mechanics* (2014) 52(3):767-780.
47. Li P, Liu P, Liu Z, Liu W. Experimental and numerical study on the heat transfer and flow performance for the circular tube fitted with drainage inserts. *International J Heat Mass Transf*. 2017;107:686-696. [\[CrossRef\]](#)
48. Dong C, Hibiki T. Heat transfer correlation for two-component two-phase slug flow in horizontal pipes. *Applied Therm Engineering*. 2018;141:866-876. [\[CrossRef\]](#)
49. Tu X-C, Wu Y, Kim H-B. Improvement of two-phase flow distribution in the header of a plate-fin heat exchanger. *International J Heat Mass Transf*. 2018;123:523-533. [\[CrossRef\]](#)
50. Karupphasamy M, Saravanan R, Chandrasekaran M, Muthuraman V. Numerical exploration of heat transfer in a heat exchanger tube with cone shape inserts and Al₂O₃ and CuO nanofluids. *Mater Today Proc*. 2020;21:940-947. [\[CrossRef\]](#)
51. Yadav S, Sahu SK. Heat transfer augmentation in double pipe water to air counter flow heat exchanger with helical surface disc turbulators. *Chem Eng Process Process Intensif*. 2019;135:120-132. [\[CrossRef\]](#)
52. Xiong Q, Izadi M, Shokri rad M, Shehzad SA, Mohammed HA. 3D numerical study of conical and fusiform turbulators for heat transfer improvement in a double-pipe heat exchanger. *International J Heat Mass Transf*. 2021;170:120995. [\[CrossRef\]](#)
53. Bashtani I, Esfahani JA, Kim KC. Effects of water-aluminum oxide nanofluid on double pipe heat exchanger with gear disc turbulators: A numerical investigation. *J Taiwan Inst Chem Eng*. 2021;124:63-74. [\[CrossRef\]](#)
54. Khetib Y, Sedraoui K, Melaibari AA, Alsulami R. The numerical investigation of spherical grooves on thermal-hydraulic behavior and exergy efficiency of two-phase hybrid MWCNT-Al₂O₃/water nanofluid in a parabolic solar collector. *Sustain Energy Technol Assess*. 2021;47:101530. [\[CrossRef\]](#)
55. Boure JA, Bergles AE, Tong LS. Review of two-phase flow instability. *Nucl Eng Des*. 1973;25(2):165-192. [\[CrossRef\]](#)